https://doi.org/10.5194/egusphere-2026-6107
Preprint. Discussion started: 22 November 2026
© Author(s) 2026. CC BY 4.0 License.

Insights on Convective–Stratiform Designation and Its Ambiguity from Radar Wind Profilers at Darwin, Australia

Scott E. Giangrande[1], Christopher R. Williams[2], Israel Silber[3], and Alain Protat[4]

[1]Environment and Energy Division, Brookhaven National Laboratory, Upton, NY, USA
[2]Aerospace Engineering Sciences Department, University of Colorado, Boulder, CO, 80303, USA
[3]Atmospheric and Earth Sciences Division, Pacific Northwest National Laboratory, Richland, WA, 99352, USA
[4]Bureau of Meteorology, Melbourne, Victoria, Australia

Correspondence to: Scott E. Giangrande (sgrande@bnl.gov)

Abstract. Convective–stratiform (C-S) classifications are widely used in deep convective cloud remote sensing studies and model evaluation using observations. Most C-S classification (CSC) relies on a limited set of canonical signatures. Dual-frequency wind profiler observations collected at Darwin, Australia, provide a unique opportunity to constrain C-S designation by directly retrieving hydrometeor fall speed Vt, which may better identify the presence of faster falling, convective-processed media. Here, Random Forest (RF) methods are used to compare how well simple conventional radar features reproduce these Vt-informed classifications.

Reflectivity factor (Z) properties associated with the vertical structure of precipitation outperform simpler measures of precipitation intensity. Combinations of Z-based characteristics often exceed 80% skill across multiple C-S predictor sets. Mean Doppler velocity (MDV) provides additional discriminatory value when strong vertical motions (>2-3 ms^{-1}) are identified above the melting level, with MDV pairings often exceeding 90% skill in recovering C-S regimes. Analogous tests using Vt provide higher performance, though genuine Vt insight aloft provides negligible improvement over other Doppler fields once additional predictors are considered. These results suggest that direct Vt insight is not a requirement for streamlining CSC model-observational evaluation. Further, most RF predictions strongly favor one C-S class, with such decisive predictions agreeing with our reference >95% of the time. Disagreement exceeds 30% among less-decisive predictions, where characteristic C-S structures also become less distinct. This study considers RF prediction ambiguity as one means for reconciling binary C-S designations with the fluid nature of these precipitation states.

1 Introduction

Convective-stratiform (C-S) partitioning is useful to a range of observational applications in deep convection and various model-observation evaluation activities (e.g., Churchill and Houze, 1984; Steiner et al., 1995; Williams et al., 1995; Tokay and Short, 1996; Biggerstaff and Listemaa, 2000; Lang et al., 2003; Powell et al., 2016; Dixon and Romatschke, 2022). Such classifications exploit the contrasting dynamical-microphysical nature of convective and stratiform precipitation processes,

https://doi.org/10.5194/egusphere-2026-6107
Preprint. Discussion started: 22 November 2026
© Author(s) 2026. CC BY 4.0 License.

including expected differences in rainfall rates, hydrometeor populations, vertical air motions and latent-heating structure (Gamache and Houze, 1983; Houze, 1989; Johnson et al., 1999; Bringi et al., 2003; Shige et al., 2004; Schumacher et al., 2004; 2007; Tao et al., 2019). For radar-based hydrological applications or vertical air velocity retrieval, an ability to identify convective regions often underpins drop size distribution or fall speed parameterization for these fundamental measurements (e.g., Giangrande et al., 2008a; 2014; 2026; Wang et al., 2018; 2019; 2020a). Although the use of C-S classification (CSC) methods has become routine, they are inherently approximate for deep convective systems where precipitation and associated processes evolve along a continuum (e.g., Houze, 1997). Such separations are often inferred from the use of simple microphysical radar proxies, rather than basing CSC on observations of the underlying cloud dynamics that remains difficult to measure (e.g., Williams et al., 1995; Atlas et al., 2000). Often, confidence in existing CSC relies on factors such as: (i) identifying familiar radar process signatures (e.g., a reflectivity factor, Z, "bright band" and aggregation/melting signatures; Fabry and Zawadzki, 1995; Kumjian et al., 2016), (ii) whether classifications behave as physically (or expert) expected, or (iii) whether classifications agree with an existing CSC method (e.g., Anagnostou, 2004; Yang et al., 2019; Ghada et al., 2022). Independent validation is challenging for most radar classification topics; examples such as dual-polarization "hail" detection paired with surface verification have demonstrated relatively high probabilities of detection with low false-alarm rates for well-defined signatures (Heinselman and Ryzhkov, 2006). Equivalent validation is considerably less definitive for CSC, and less is known about expected method accuracy or which radar quantities provide the most useful discriminatory information.

Profiling radars previously deployed at Darwin, Australia provide an opportunity to examine these ideas and potential implications from a vertically pointing and multi-frequency perspective not available to prior C-S studies. Building on the longstanding development of dual-frequency and longer-wavelength capabilities for Darwin profiling radars (e.g., Protat and Williams, 2011; Williams, 2012; Schumacher et al., 2015), it is possible to directly retrieve unattenuated estimates of the vertical air motion in storms, as well as bulk hydrometeor fall speed in deep convective contexts to higher altitudes (e.g., Giangrande et al., 2026). Here, Darwin observations allow traditional radar moments to be compared directly with storm kinematics. For retrieval-oriented applications in more intense or organized cloud settings, a useful definition of "convective" precipitation is the presence of convectively processed hydrometeors (e.g., lofted liquid, graupel, or hail) associated with enhanced rainfall rates, vertical air motion or fall speed variability. As such, Darwin observations can serve as an important baseline against which to test C-S concepts relevant to many retrieval-oriented needs.

Prior radar-based C-S studies have emphasized canonical Z-based and/or scanning weather (longer wavelength) radar signatures, such as regions having Z higher than a threshold, or criteria related to the texture in Z fields. This is practical given widespread operational network usage and data availability. However, it is unclear whether these or similar common radar concepts are uniquely informative to CSC. Identifying alternate proxies may be beneficial for model evaluation or remote-sensing applications when traditional signatures may be absent, biased, or not well-simulated. A primary motivation for this study is to examine the value of conventional radar moments, as commonly applied to distinguishing precipitation regimes

https://doi.org/10.5194/egusphere-2026-6107
Preprint. Discussion started: 22 November 2026
© Author(s) 2026. CC BY 4.0 License.

within deep convection. We further consider how effectively available radar information supports individual C-S distinctions, particularly for conditions where less-decisive designations may impact radar retrievals or radar–model comparisons. Although this effort is directed toward profiling radar observations and scales, several concepts may be relatable to scanning radar or satellite-based CSC that employ similar quantities at different spatial/temporal scales.

These objectives are addressed using profiler observations collected in Darwin, Australia by considering the predictive capability of radar fields. We use supervised machine-learning (ML) methods as a primary means for quantifying regime differences. This is done through a controlled set of comparisons drawn from conventional and select profiler- and Darwin specific radar diagnostics. Tests are aimed at identifying simpler quantities, absolute and/or relative levels, and other integrated behaviors from profiler observations informative to CSC. In Section 2, we introduce the Darwin dataset and our methods. Results on the predictive capability associated with different Darwin radar profile inputs, as well as select time-height displays for more generalized capabilities and ambiguities of these ideas in deep convective contexts are found in Section 3. A discussion on some of the implications of these methods is given in Section 4.

2 Dataset and methods

This study uses observations collected by the dual-frequency (50- and 920-MHz) Darwin radar wind profiler systems (e.g., Protat and Williams, 2011) during the 2005-2006 Australian monsoon season (November to April). These profiler datasets have been extensively studied for retrieval of vertical air motion, precipitation microphysics, and other applications relevant to tropical deep convection (e.g., Williams, 2012; Kumar et al., 2015; 2016; Schumacher et al., 2015; Giangrande et al., 2026). Detailed descriptions of the Darwin instruments, calibration, and dual-frequency retrieval methodology are found in those previous studies. Our study retains 36 events, where an event is defined as any day having at least 20 minutes of convective overpass as based on the CSC we define in Section 2.1. Events typically featured a mixture of isolated ordinary to organized convection with widespread stratiform precipitation. The classification algorithm in Section 2.1 is informed by unique Darwin dual-frequency profiler insight, and acts as our reference for ML applications introduced in Section 2.2.

2.1 Darwin convective-stratiform reference classification

The reference CSC algorithm adopts concepts from Geerts and Dawei (2004), Lerach et al. (2010) and Giangrande et al. (2013, 2026) with a few modifications. It performs a series of checks based on 920-MHz profiler quantities at a gate-by-gate level (105 m range resolution): reflectivity factor Z, mean Doppler velocity MDV, spectrum width SW, and a 5-gate standard deviation of Z, SD(Z). We capitalize on additional quantities available from the 50-MHz profiler to include the dual-frequency vertical air motion retrieval Va (available at 315 m range resolution), as well as a reflectivity- (or power-) weighted hydrometeor fall speed Vt that is estimated as the residual of the 920-MHz profiler MDV field and the Va retrieval (e.g., Protat and Williams, 2011; Giangrande et al., 2026). These Vt estimates can be interpreted as a bulk radar-volume property, sensitive

https://doi.org/10.5194/egusphere-2026-6107
Preprint. Discussion started: 22 November 2026
© Author(s) 2026. CC BY 4.0 License.

to the presence of higher density or faster falling mixed-phase media. The presence of such media is consistent with Houze (1997) expectations for convective precipitation, and is relevant for radar-based retrievals that require appropriate fall speed corrections. Media advected into transitional regions may retain convective fall speed characteristics even after the surrounding environment or Z structure has shifted towards stratiform (e.g., Powell et al., 2016). From a profiling radar retrieval perspective, these locations may still require "convective" fall speed treatments until such signatures are no longer distinguishable. Following previous Darwin studies, we use profiles collected from 1.7 to 8.0 km above ground level (agl) and gates having Z > 20 dBZ to ensure applicability of dual-frequency profiler methods at altitude. We further exclude gates where the 50-MHz profiler and its air motion retrievals are unavailable or retrieve unrealistic results (i.e., Va > 50 ms^{-1}). Columns also need to contain at least one radar echo exceeding 30 dBZ to be included.

The algorithm employs several steps that progressively isolate and quality-control the columns that make up our reference dataset. The first step is to separate likely "Bragg" or other nonmeteorological echo from precipitation. This step flags and excludes gates at low-altitude (below 4 km), Z < 30 dBZ regions having a narrow range of |MDV|, Vt < 1.0 ms^{-1}, and low spectrum width (for the Darwin 920-MHz profiler, typically < 3 ms^{-1}). Second, we identify potential "bright band" gates (e.g., Fabry and Zawadzki, 1995; Giangrande et al., 2008b) and filter in time-height around these locations. For this step, a simple check identifies gates within a relatively wide range of Z (25 < Z < 50 dBZ) associated with elevated SD(Z) > 2 dBZ as evidence of melting aggregates below a pre-defined melting level (for the Darwin dataset, fixed at 5 km agl). These data points serve as input to a two-pass boxcar filtering: The first is a 5x5 time-height noise reduction filter that requires at least 7 surrounding gates being "bright band" for the point to be retained. The second is an iterative 5 × 5 neighborhood filter that allows newly identified bright band gates to contribute to subsequent filtering. A point is retained when at least 11 surrounding gates are identified as "bright band". This second pass preferentially extends coherent bright band regions in time while limiting vertical growth.

Our last step is to apply a binary label that assigns profiler columns as "convective" or "stratiform". Stratiform is the default label for all gates within any column, whereas convective gates are assigned to gate locations having elevated Z > 35 dBZ and spectrum width > 2 ms^{-1}. Additional checks are performed above the melting level to identify gates having larger Vt > 2.5 ms^{-1} associated with convective media and/or related fall speeds for those volumes. Columns are promoted to "convective" provided that those columns have a minimum of 5 convective 920-MHz gates and the absence of a bright band. Columns containing previously identified bright band regions are excluded and assigned as "stratiform" columns. Thus, columns will not be labelled as "convective" even if media aloft is sufficiently faster falling, provided a bright band was previously identified. Some implications of such choices for reference classifications will be discussed in Section 4. In Figure 1, we provide an example of profiler observations and classifications for an event on 18 February 2006. For this dataset, the 36 precipitation events contained 6,262 valid precipitation columns, with 2,042 (32.6%) convective and 4,220 (67.4%) stratiform classifications.

https://doi.org/10.5194/egusphere-2026-6107
Preprint. Discussion started: 22 November 2026
© Author(s) 2026. CC BY 4.0 License.

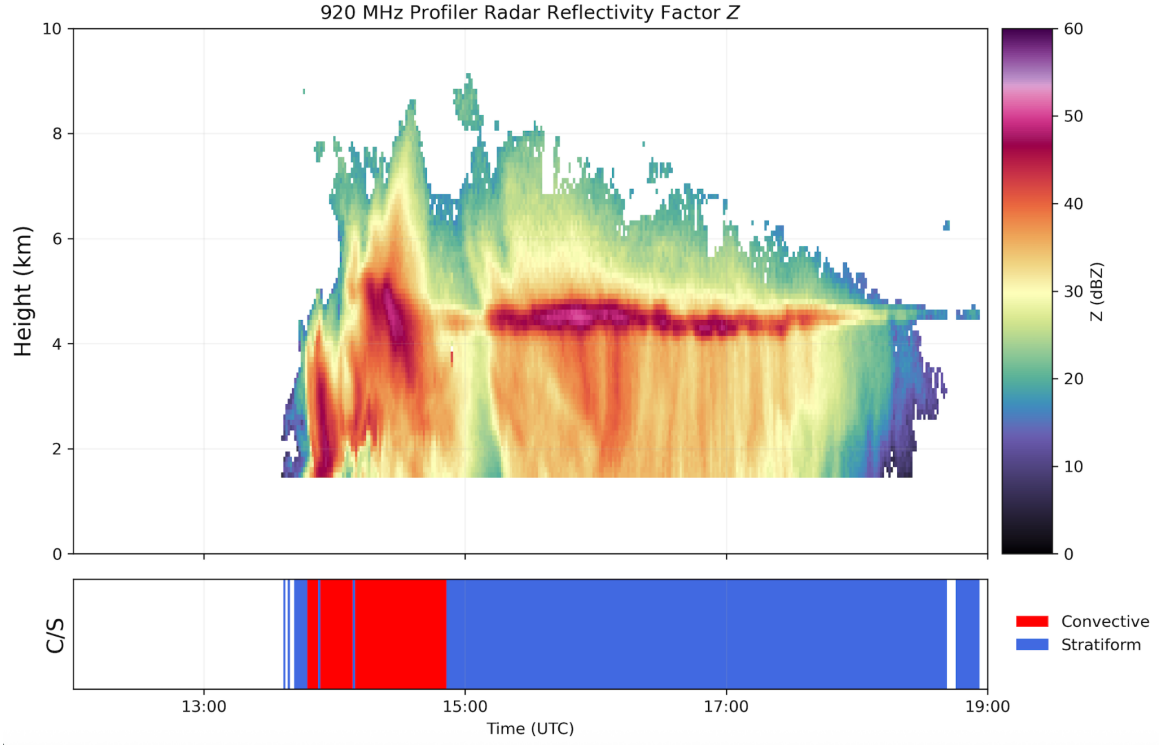


Figure 1: An example of Darwin 920 MHz Profiler radar reflectivity factor Z (top) and an associated convective and stratiform rain reference echo classifications for an event on 18 February 2006.

2.2 ML predictor design and skill metrics

C-S designations in Section 2.1 serve as our reference labels for this study. We adopted Random Forest (RF; Breiman, 2001) and Extremely Randomized Trees (ExtraTrees; ET; Geurts et al., 2006) classifiers to investigate how well radar-derived features reproduce those classifications. Ensemble tree methods require relatively few assumptions regarding predictor distributions or scaling, represent nonlinear relationships between variables, and have demonstrated robust performance for meteorological applications (e.g., Gagne et al., 2014, 2017; Wang et al., 2020b; Mecikalski et al., 2021). RF methods are also computationally efficient and well suited to the modest Darwin dataset sample size combined with the low-dimensional predictor combinations (features) considered. As RF and ET produced nearly similar performance, we only report RF results hereafter.

The RF classifiers we use are available within the scikit-learn Python package (Pedregosa et al., 2011). The hyperparameters we use include a maximum tree depth of 8, 50 estimators (trees), and three-fold GroupKFold cross-validation, ensuring that complete events were withheld between training and validation subsets. Predictions for each withheld event group are referred to as "out-of-fold" predictions; thus, each reported prediction is generated by an RF that was not trained using that event. Only minor improvement was found for larger hyperparameter values compared with the increased computational cost and risk for

https://doi.org/10.5194/egusphere-2026-6107
Preprint. Discussion started: 22 November 2026
© Author(s) 2026. CC BY 4.0 License.

overfitting. Performance for this study is primarily communicated using balanced accuracy, which weights the ability to correctly identify each class equally despite differences in class frequency. For a binary CSC approach, a balanced accuracy of 0.5 represents chance-level discrimination, whereas 1.0 represents perfect classification. A balanced accuracy of 0.85 can be interpreted as approximately 85% skill after accounting equally for the ability to identify C-S columns. As a complementary measure of performance, we report the macro-averaged F1 score (macro-F1), which incorporates the precision and recall associated with each class before weighting the C-S classes equally. Macro-F1 provides an indication of whether successful CSC is accompanied by erroneous assignments of the opposing class.

Perfect classification is not expected because the reference designations themselves carry uncertainty and profiling radar cannot sample the full spatiotemporal structure of evolving C-S precipitation. Reported performance should be interpreted as representative only of Darwin tropical deep convection and its reference classifications rather than as an immutable property of a particular radar predictor. Performance for individual events will vary beyond the cross-validation averages we report (see also, Section 4).

As an additional metric, we use the RF class probabilities to define a prediction-ambiguity qualifier based on the class-probability margin,

$$A_i = 1 - |2p_i - 1| \quad (1)$$

where p_i is the RF probability assigned to the convective class. This formulation assumes that binary predictions approaching equal class probabilities are increasingly uncertain. A value of 0 indicates the strongest preference for one classification, whereas a value of 1 indicates the highest ambiguity between C-S classes. This field should not be interpreted directly as "correctness"; A_i reflects how decisively the RF favors one C-S class rather than whether that prediction agrees with our reference. Low ambiguity does not guarantee agreement, nor does high ambiguity imply disagreement, although more-decisive predictions should generally exhibit greater agreement. Section 3.3 evaluates this relationship for the Darwin dataset.

Our RF experiments use a set of scalar radar features obtained from each precipitation column. These represent different aspects of echo intensity, vertical extent, profile structure, and Doppler velocity behavior. Our tests are not intended to be exhaustive, though we include several physically interpretable quantities common for scanning and vertically pointing radars. Reflectivity factor-based predictors include the Z at a 2-km reference altitude, which in the case of Darwin represents a "rain" reference level given typical melting levels (4-5 km agl). If no echoes are present at the 2 km altitude, this value is assigned as 0 dBZ (to accommodate the RF requirement of finite training sample sets). Other features we test are the maximum Z within each column, as well as the height of this maximum Z. Echo-top heights (ETH) are found using 20-, 30-, and 40-dBZ thresholds; ratios among these heights are estimated to add simple measures of relative profile structure. The ETHs (and/or ratios therein) are assigned and/or calculated using a value of 0 km if no echo matching that level is found in the column. We also consider additional measures such as column-integrated Z (in linear units, this is proportional to vertically integrated

https://doi.org/10.5194/egusphere-2026-6107
Preprint. Discussion started: 22 November 2026
© Author(s) 2026. CC BY 4.0 License.

liquid "VIL" and herein referred to as such), integrated Z above 5.5 km agl, and height- or air density-weighted integrated-Z quantities (e.g., Kumar et al., 2016).

Simple MDV-derived predictors may provide significant information distinct from Z-based features. We consider a reference for the maximum absolute MDV, and its corresponding altitude. Although dual-frequency MDV differences are related to median drop size (e.g., Tian et al., 2007; Giangrande et al., 2012), single-frequency MDV typically varies little in rain below the melting level, limiting its expected C-S discriminatory insight. Here, we also define a binary "|MDV| Aloft" feature to identify columns containing MDV > 3 ms^{-1} above 5.5 km agl. This |MDV| threshold is consistent with "convective" media motions exceeding typical stratiform ice fall speeds (e.g., Houze, 1993) and similar values have been adopted by profiler CSCs (see also, Section 2.1, |MDV| > 2.5 ms^{-1}). Sensitivity tests (not shown) indicate that C-S predictions did not vary much between threshold ranges of 2.5 ms^{-1} to 3.25 ms^{-1}. Our usage assigns a column a score of 1 if these motions are present. The 5.5-km altitude is a simplification allowed by the relatively stable melting level found at Darwin throughout the monsoon season. Approximately 15% of our columns do not contain radar echoes above 5.5 km, which breaks down into roughly 10% of convective columns and 17% of stratiform columns for our reference classification. This binary approach will place a value of 0 for these instances to meet RF training requirements.

Figure S1 summarizes the relationships among the radar features using a Pearson correlation matrix. Several features are knowingly correlated because they represent related aspects of column intensity or vertical structure. Our analysis in Section 3 starts by evaluating these features individually. We then subsequently evaluate all possible two- and three-feature combinations using the same RF configuration and event-based cross-validation. Comparison among these experiments provides a controlled measure of predictive information gained as radar characteristics are combined.

Finally, we perform a sensitivity experiment in which the aforementioned binary |MDV|-Aloft feature is replaced by an analogous one based on Vt retrievals (Vt > 2.5 ms^{-1}). Darwin Vt is less independent as a predictor, since knowledge of stronger fall speeds in the column builds additively on other radar observations to our reference CSC (Section 2.1, Vt > 2.5 ms^{-1}). We maintain this check as a partial benchmark, rather than as part of a realistic profiling radar predictor discussion. However, comparisons between MDV- and Vt-based experiments, based on their similar usage, are quite relevant to single versus dual-frequency C-S classification fidelity and its subsequent role in profiler air motion retrievals. Additional tests also consider a comparable SW indicator, defined by the presence of SW exceeding 2.0 ms^{-1} above 5.5 km agl. As with Vt and MDV, the coupled presence of large Z and SW helps define "convective" columns. Of these, SW is the least intuitive (or most complex) observable, because it is strongly influenced by various region- and regime-dependent physical process and system differences, and hence, necessitates a more subjective threshold assessment. As such, while we do not include SW results as part of the primary predictor suite, we will reference SW throughout the study.

https://doi.org/10.5194/egusphere-2026-6107
Preprint. Discussion started: 22 November 2026
© Author(s) 2026. CC BY 4.0 License.

3 Results

3.1 Predictive capability of individual radar features

In Figure 2, we plot the balanced accuracy and macro-F1 scores obtained when individual radar features are used to reproduce the reference Darwin CSC. Performance varies considerably among the predictors, although balanced accuracy and macro-F1 generally provide similar rankings. Among the conventional Z-based radar features, the height of maximum Z provides the highest balanced accuracy of 0.81, while several other measures of echo intensity and vertical structure yield balanced accuracies near 0.75. The binary |MDV|-Aloft predictor exhibited scores ≈ 0.86, ranking the highest of all individual predictors in our primary set. A similar performance to MDV was also obtained when using checks for enhanced SW aloft, recording balanced accuracies of ≈0.85–0.87 for SW thresholds in a tested range of 2–3 ms^{-1}. By comparison, maximum Z, as well as the 20 dBZ ETH (i.e., traditional measures for precipitation intensity or cloud top height, respectively) produce lower balanced accuracies near 0.6. The Vt-Aloft benchmark gave balanced accuracy and macro-F1 values of 0.88, and was our overall strongest single-feature performer. These Doppler-based scores are notable given that 15% of columns do not contain echo above 5.5 km.

Among the individual Z-based predictors, we highlight the performance when using Z as a predictor at 2 km. For this dataset, that feature yielded scores ≈ 0.75. This predictor partially resembles a traditional Steiner et al. (1995) C-S approach that uses lower-level Z fields, and the result provides a confirmation for the importance of a simple “rain” intensity reference. Several Z-based predictors that communicate the vertical location or extent of stronger echoes provide similar or higher skill, including the 30-dBZ echo-top height. This follows physically from the lofting of liquid or more intense precipitation in convection, but these connections may deteriorate as a function of lifecycle sampling and other considerations. The physical basis for differences among individual predictors is considered further in Section 4.

https://doi.org/10.5194/egusphere-2026-6107
Preprint. Discussion started: 22 November 2026
© Author(s) 2026. CC BY 4.0 License.

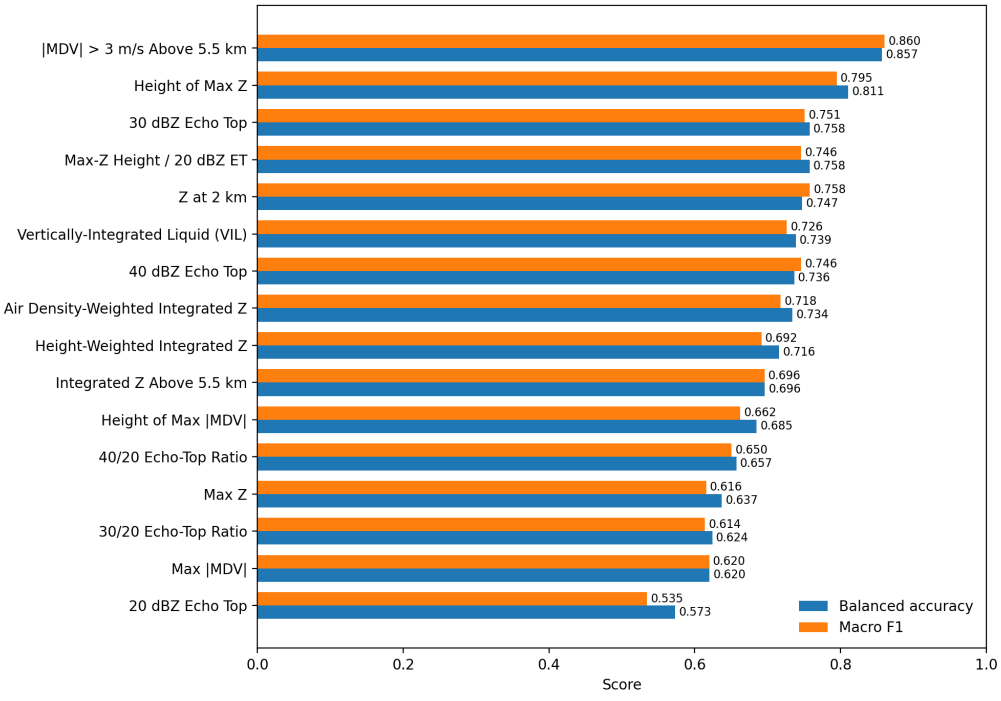


Figure 2: Out-of-fold balanced accuracy and macro-F1 scores for C-S classifications using individual radar features. Scores are ordered by balanced accuracy.

3.2 Predictive capability from combined radar features

In Figure 3, we extend these tests to consider all possible two-feature combinations. Balanced accuracy and macro-F1 suggest similar patterns across the pairings. Approximately 75% of our 120 two-feature combinations improved relative to the better-performing of their constituent predictors. The highest scores are associated with combinations that include the |MDV|-Aloft predictor, with scores ≈ 0.9 when paired with canonical features such as the Z at 2 km. Marked improvement was not only limited to combinations containing |MDV|-Aloft; several Z-only pairs achieve success > 0.8, typically the combinations pairing the height of maximum Z with measures of column-integrated Z. Here, combining information from different parts of the profile helps distinguish intense convection from strong melting-layer enhancements (see also, Section 4). Figure 4 expands upon these results by displaying balanced accuracy for our set of two-feature combinations (a macro-F1 heatmap is found in Figure S2). Note that diagonal values on Figure 4 also correspond to those found in Figure 2. As before, combinations that include velocity aloft consistently outperform others. Nevertheless, the overall heatmap further suggests that solid performance is not strongly dependent on any single selected metric, and can still be obtained without Doppler signatures.

https://doi.org/10.5194/egusphere-2026-6107
Preprint. Discussion started: 22 November 2026
© Author(s) 2026. CC BY 4.0 License.

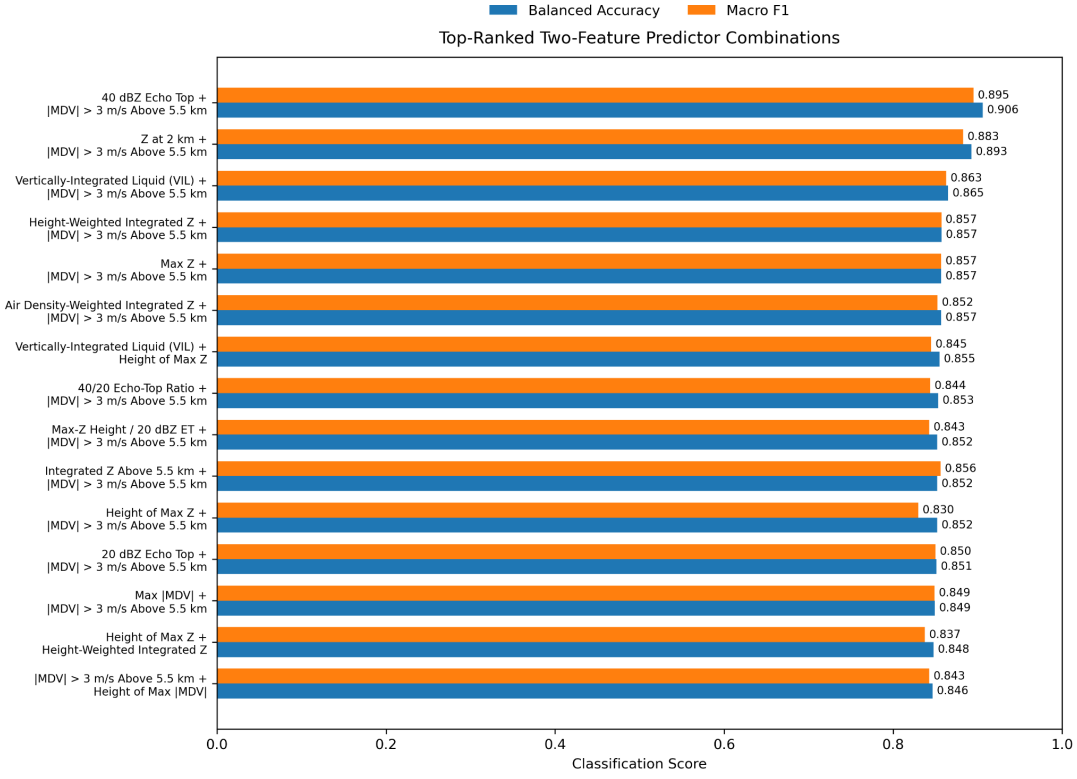
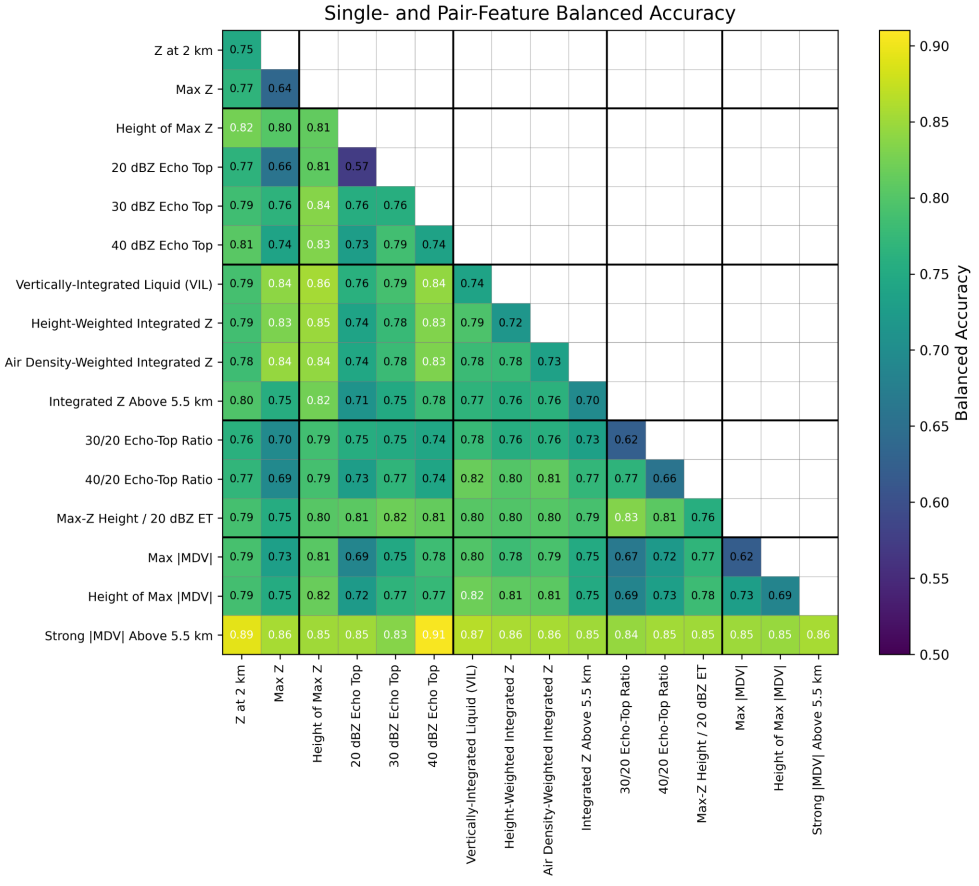


Figure 3: Top-ranked two-feature C-S predictor combinations (ranked by balanced accuracy), with corresponding macro-F1 scores.

The addition of a third predictor provides comparatively little improvement (Figure 5). The highest-ranked triplets yield balanced accuracies ≈ 0.91, many suggesting equivalent performance to constituent pairs (e.g., within standard deviations). Replacing |MDV|-Aloft with a similar Vt concept increases the highest two-feature scores to ≈ 0.92, with our highest three-feature combinations similarly topping out at ≈ 0.92. The suggestion is that having genuine Vt insight provides little additional improvement once a more complete set of predictors are considered. This implies our classifications may have approached practical limitations imposed by profiler sampling and these simple feature designs (see also, Section 4).

https://doi.org/10.5194/egusphere-2026-6107
Preprint. Discussion started: 22 November 2026
© Author(s) 2026. CC BY 4.0 License.



260

Figure 4: Heatmap of balanced accuracy for individual and two-feature RF classifications. Diagonal entries show single-feature scores and off-diagonal entries show the corresponding feature-pair performance.

https://doi.org/10.5194/egusphere-2026-6107
Preprint. Discussion started: 22 November 2026
© Author(s) 2026. CC BY 4.0 License.

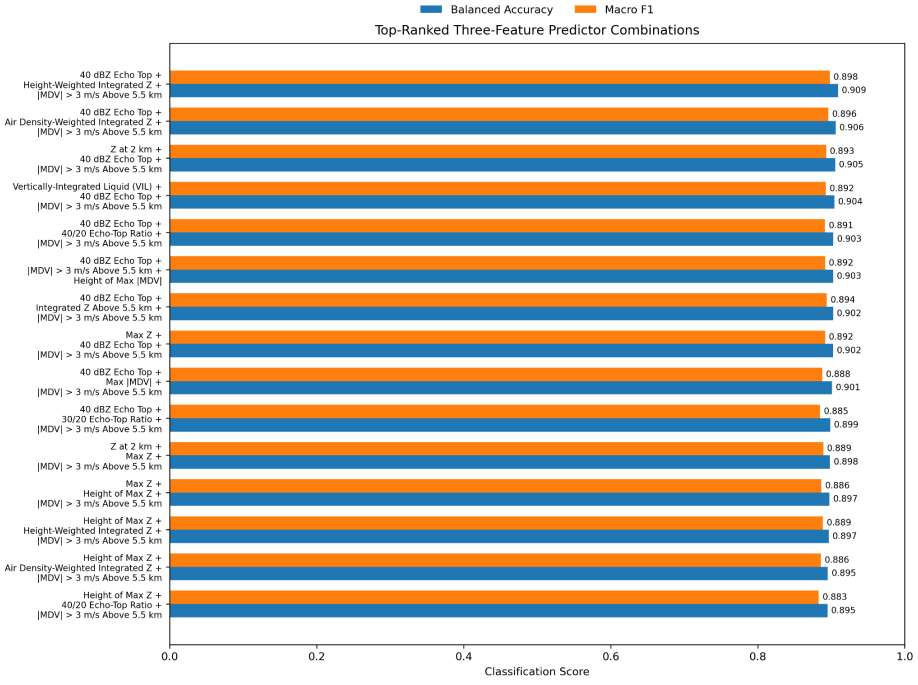


Figure 5: Top-ranked three-feature C-S predictor combinations according to balanced accuracy, with corresponding macro-F1 scores.

3.3 Event-level C-S prediction and ambiguity

In Figure 6, we provide an event-level example of C-S predictions for the Darwin event on 18 February 2006. For this display, we select one of the higher-performing three-feature combinations (40-dBZ echo-top height, height-weighted integrated Z, and |MDV|-Aloft) to serve as our RF predictors. Profiler moments are plotted along with a time-series of our reference C-S behavior. Our out-of-fold RF C-S predictions and the prediction ambiguity A_i are also plotted. The event featured an organized convective system that passed over the profilers between 14 and 18 UTC, capturing a deep convective line trailed by widespread stratiform exhibiting a pronounced "bright band" Z enhancement. Additional examples of event-level behaviors can be found in Figure S3.

Elevated A_i values frequently occur in the "transitional" zones following convective cores, as evident with the principal C-S transition around 15 UTC. Higher A_i is also found within the predominantly stratiform region prior to 16 UTC, where this RF implementation intermittently predicts convective columns amid the most pronounced Z "bright band" signatures potentially associated with a period of increased aggregation aloft. These locations show where elevated ambiguity and disagreement with the reference coincide. For example, portions of the transitional zone prior to 15 UTC exhibit relatively large A_i even when the predicted and reference CSC agree. Integrated Z fields struggle with the most intense bright band signatures, and this example highlights where three-feature combinations do not always add value over a two-feature variant.

https://doi.org/10.5194/egusphere-2026-6107
Preprint. Discussion started: 22 November 2026
© Author(s) 2026. CC BY 4.0 License.

The complete set of Darwin out-of-fold predictions provides a broader context for interpreting prediction ambiguity and its relationship to CSC performance. Low-ambiguity classifications dominate our predictions across this dataset and, expectedly, are also strongly associated with agreements with our Darwin reference. For example, if we select an upper A_i cutoff value of 0.25 to identify relatively unambiguous predictions (i.e., the RF assigns ≥ 87.5% probability to one C-S class), approximately 96% of those columns agree with our reference classification. This 0.25 threshold separates a population for which disagreement remains consistently low from a region where disagreement begins increasing rapidly (Figure 7). Overall, low-ambiguity conditions that agree with our reference account for nearly 80% of precipitation columns. Another 13% of our columns also agree with our reference despite exhibiting an $A_i > 0.25$; as before, an elevated A_i does not imply disagreement with our reference. Nonetheless, "disagreement" is increasingly concentrated at larger A_i values for our dataset. Approximately 6% of columns have an ambiguity > 0.25 and disagree with our reference classification; these situations account for two-thirds of our total disagreements.

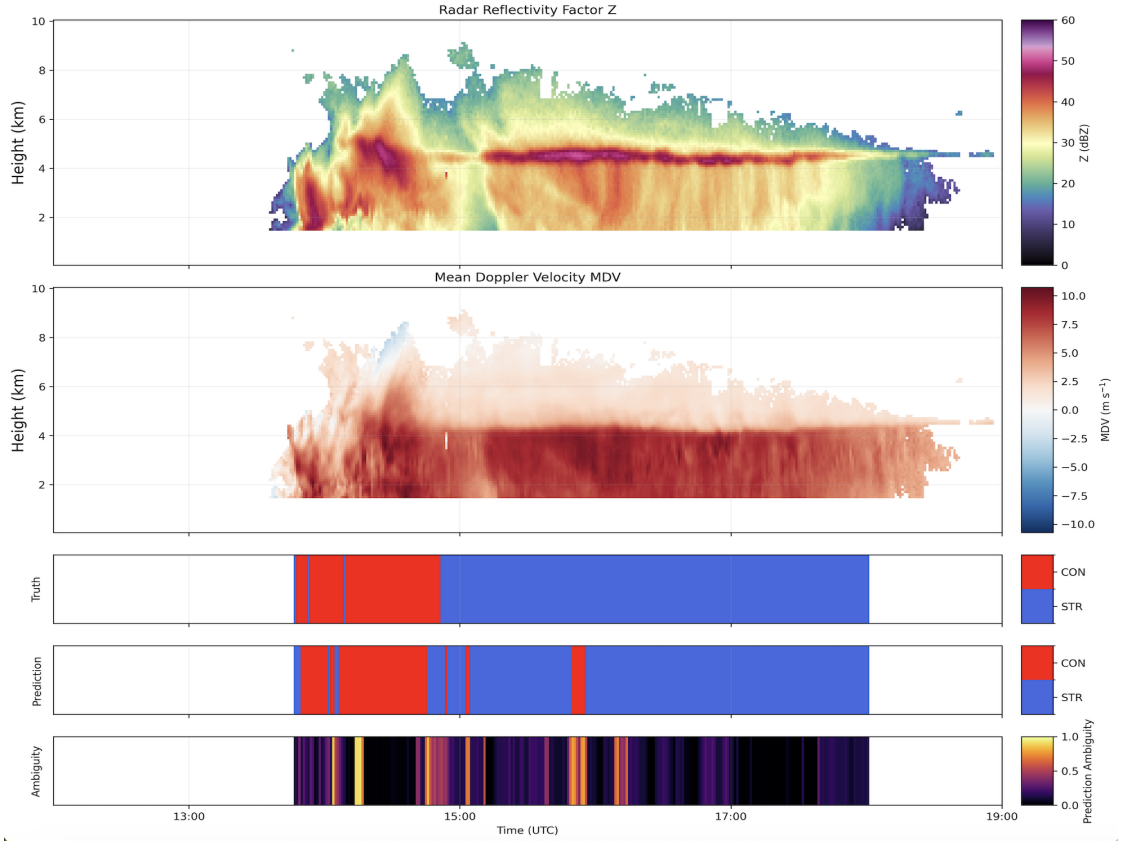


Figure 6: Darwin profiler observations and RF C-S classifications for the 18 February 2006 event. Panels show time–height (i) reflectivity factor Z and (ii) mean Doppler velocity MDV (positive is downward). Bottom panels display (iii) the reference C-S designation, (iv) our out-of-fold RF prediction using [40-dBZ echo-top height, height-weighted integrated Z, and |MDV|-Aloft], and (v) prediction ambiguity A_i.

https://doi.org/10.5194/egusphere-2026-6107
Preprint. Discussion started: 22 November 2026
© Author(s) 2026. CC BY 4.0 License.

300

Our associations here depend in part on the selected A_i value. Darwin predictions disagree less than 2% of the time for $A_i \leq 0.1$ contexts. However, disagreement increases to >30% once we consider A_i values much beyond our 0.25 threshold (Figure 7). Recall, A_i maps directly to the RF class probability; the value approaches 1 as the probabilities converge toward a chance-level 0.5 preference between C-S classes. As such, increasingly large A_i identifies conditions where the predictors provide
305 progressively weaker support for either designation. This relationship also differs between C-S classes: above $A_i = 0.25$, more than 30% of columns predicted as convective are stratiform according to our reference, whereas stratiform predictions remain comparatively accurate until the highest-ambiguity ranges.

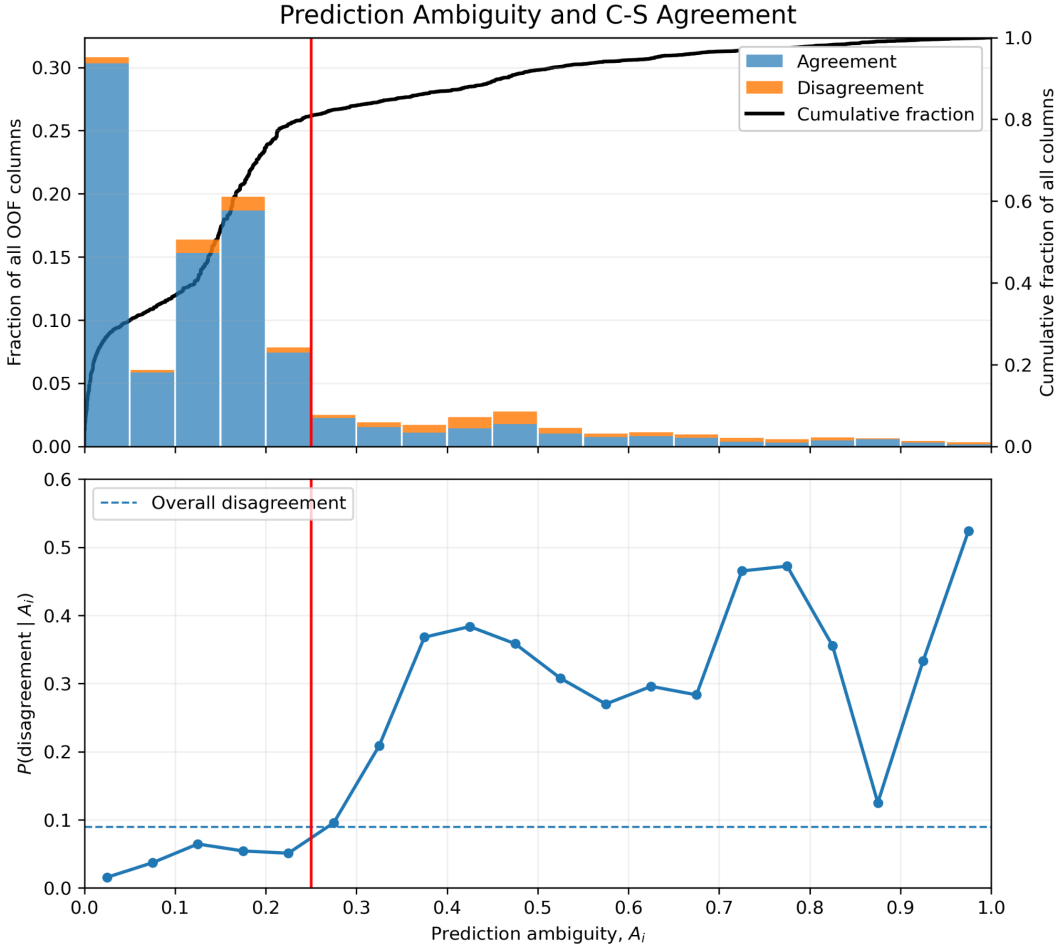
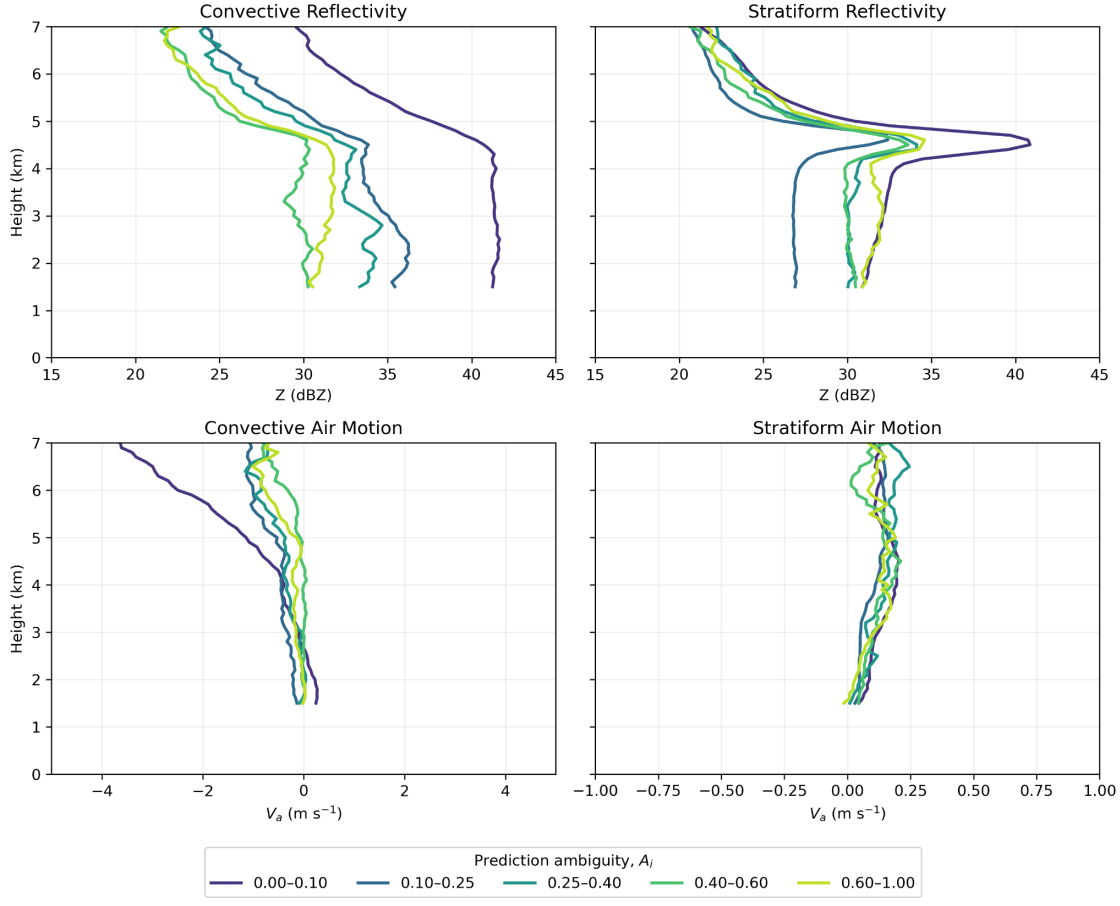


Figure 7: Prediction ambiguity Ai for Darwin out-of-fold (OOF) C-S classifications. (a) Fraction of precipitation columns partitioned
310 **according to agreement or disagreement with the Darwin reference classification. (b) Probability of disagreement with the reference classification as a function of Ai; the horizontal dashed line indicates the overall disagreement rate. The solid red line denotes the Ai = 0.25 reference choice.**

https://doi.org/10.5194/egusphere-2026-6107
Preprint. Discussion started: 22 November 2026
© Author(s) 2026. CC BY 4.0 License.

315 In Figure 8, we plot composite median Z and Va profiles for the reference C-S population across five A_i ranges from the higher-performing three-feature RF configuration (corresponding mean profiles are found in Figure S4). Lower-ambiguity convective columns exhibit more intense Z throughout the column and stronger upward Va aloft. These profile signatures weaken at larger A_i, however the composite profiles still retain convective characteristics. In contrast, stratiform profiles exhibit melting layer Z signatures across all A_i ranges, with median/mean peak-to-rain enhancements decreasing toward higher
320 ambiguity (i.e., weaker "bright band" enhancement). Unsurprisingly, stratiform air motion profiles are comparatively weak and predominantly downward. Mean Va composite profiles exhibit stronger upward air motions aloft than their corresponding median profiles. Section 4 will further consider the physical contexts associated with C-S prediction ambiguity and the implications for practical profiler applications.



325 **Figure 8: Median profiles of Z and Va for our reference convective and stratiform populations, composited across five ranges of prediction ambiguity from a higher performing three-feature RF prediction. Darker colors indicate lower prediction ambiguity.**

https://doi.org/10.5194/egusphere-2026-6107
Preprint. Discussion started: 22 November 2026
© Author(s) 2026. CC BY 4.0 License.

4 Discussion

4.1 Radar information supporting C-S distinctions

Radar CSCs are inherently approximate owing to the evolving nature of convective and stratiform process regimes found in deep convective clouds. Nevertheless, distinguishing such regimes has become a practical staple of model evaluation, and has found use in applications where CSC informs rainfall, fall speed, or other retrieval assumptions. A central question this study asks is how effectively the information available from radar measurements supports such C-S distinctions given the fluid nature of process transitions. For Darwin observations, our results suggest that even a small number of relatively simple radar properties, including several traditional staples, often perform well. Simple individual predictors based on Doppler information aloft returned balanced accuracies as high as ≈ 0.85-0.88, while two-feature combinations exceeded 0.90. Better performances were however not limited solely to the use of profiler Doppler moments, as useful discrimination was also recovered from several conventional Z column properties. More broadly, our results suggest that useful C-S information is distributed across several radar characteristics rather than uniquely tied to one canonical signature (i.e., "faster" motions aloft). Combining complementary predictors improves discrimination when they provide sufficiently independent information, whereas performance gains diminish as additional features increasingly communicate redundant aspects of the precipitation column.

The performance of the Z-based features is consistent with the longstanding utility of conventional radar heuristics for C-S classification. The simplest of these – the 2-km "rain" reference level Z – produced balanced accuracy and macro F1 values close to 0.75. We often relate larger values of surface Z with more intense convective rainfall rates, and this performance provides one guideline for how adequate simple Z thresholds may be for CSC. Recent studies using Micro Rain Radar (MRR) and collocated disdrometer C-S references similarly identify lower-level Z among the more useful predictors, with their full RF model also yielding balanced accuracies near 0.8 (Ghada et al., 2022). The intended application may affect how one interprets such performances. For example, there were no "stratiform" columns in our reference that were associated with Z at 2 km > 40 dBZ, a common threshold for "convective" identification by modelers. Thus, while a simple low-level Z threshold at Darwin would not identify all convective columns, a sufficiently large value results in an effectively unambiguous "convective" designation. The modest overall score (~0.75) therefore reflects the difficulty of distinguishing C-S states when low-level Z is below 40 dBZ.

Our results further suggest that information about the vertical placement of Z signatures provides greater C-S discrimination than absolute Z intensity. Maximum Z ranked among the lower-performing predictors (≈0.64), whereas the height where this maximum occurred was our strongest Z-based feature (≈0.81). Better predictors communicate aspects of precipitation intensity and structure simultaneously. For Darwin, the height of maximum Z provides context for both the vertical development of convective precipitation and structural properties associated with canonical stratiform "bright band" signatures. Larger Z > 40 dBZ is not uniquely "convective" as similar values may be found within melting layers in stratiform regions. However, the

https://doi.org/10.5194/egusphere-2026-6107
Preprint. Discussion started: 22 November 2026
© Author(s) 2026. CC BY 4.0 License.

vertical placement of the maximum Z provides partial context for whether an enhancement reflects melting media or lofted liquid or larger convective precipitation. Other better performing predictor combinations similarly capture different aspects of precipitation intensity and structure. Such combinations still yield balanced accuracies > 0.8 without velocity information, with the highest Z-only combinations approaching 90% skill. The strong performance of several Z-only combinations suggests that only a few simple features are needed to communicate much of the C-S-relevant intensity and vertical structure of the Z profile (for Darwin events characterized by stable thermodynamic profiles, see Section 4.2). This may provide flexibility for model-observation comparisons or radar applications where particular profile characteristics are unavailable or poorly represented.

The inclusion of Doppler measurements adds an effective source of C-S information. The performance of a simple binary |MDV|-Aloft indicator (≈0.86) is solid, consistent with the design of our reference classifications that steer larger velocity signatures aloft (MDV, SW, and Vt) towards convective column classifications. These single predictor scores are respectable when accounting for the 15% of total columns that did not contain echo above 5.5 km. Predictors based on maximum MDV or the height of maximum MDV (typically, found in rain below the melting level) provided substantially less value. Additional tests that considered SW produced comparable performance to MDV. Our findings may support prior efforts such as Ghada et al. (2022), who noted that lower-level MDV, or averaged values for MDV slightly above the melting level, were not among their strongest C-S predictors. Some differences between these efforts may be attributed to how classification priorities shift if emphasizing surface-based C-S rainfall properties or designating “convective” regimes to include shallow and/or congestus clouds.

For the deep convective cases we consider, the dual-frequency Vt retrievals allow a further check of simple CSC concepts. The impact of using a direct fall speed reference was small, with individual performance rising to ≈0.88 (approximately one standard deviation improvement), whereas the best combined-feature score was ≈0.92 (within a standard deviation). Some of these differences can be attributed to instances where weak upward air motions offset the MDV signatures associated with convective fall speeds aloft. SW performance fell in between MDV and Vt, suggesting the broad advantage for having any information on elevated convective motions and/or the wider diversity of media present. Nevertheless, advantages from Vt seem to diminish as complementary predictors are included; Vt-based combinations maintain the highest scores, but differences fall within the reported variability. These results seem encouraging for single-frequency profiler applications where only MDV, or potentially SW, is routinely available – Direct Vt knowledge did not significantly shift the outcome for these forms of CSC beyond limits likely imposed by the nature of profiling observations. Where attenuation in rain is negligible, MDV or SW may therefore provide a practical substitute for direct fall speed information when applying the same C-S framework to models and observations.

https://doi.org/10.5194/egusphere-2026-6107
Preprint. Discussion started: 22 November 2026
© Author(s) 2026. CC BY 4.0 License.

4.2 Additional interpretation and practical implications of prediction ambiguity

While a possible >90% skill level seems achievable, not all classification issues are reflective of physical or process-based C-S ambiguity. Some issues instead arise from limitations of the profiling observations themselves. This includes missing (unavailable) data aloft that may lead to a preferential bias for one designation. Such sampling limitations can occur within both low- and high-ambiguity populations – missing or incomplete features that are not identified as such still may yield seemingly reasonable answers. Profiling radar will "chord" cloud structures (e.g., Borque et al., 2014), thus simple predictors may miss relevant signatures or levels. Continuity or proximity checks to identify these situations may help to recover additional skill, but achieving the most optimal of classifiers was not the goal of this effort. Initial testing of more complete profile inputs, including normalized profiles or ones missing melting layer signatures altogether (not shown) suggests that >90% skill is possible even with nonideal radar calibration, however incomplete sampling that obscures information at key profile levels remains a limiting factor.

Performance reported in this study also benefits from the environment represented by the Darwin monsoon season. The relatively stable tropical melting level allows several height- or profile structure-based features to perform consistently well as stratiform melting-layer enhancements occur over a constrained altitude range. Such relationships will be less consistent in midlatitude continental convection having greater seasonal or event-to-event variability in melting-level height, storm intensity, and vertical structure. Darwin should also not be assumed representative of all tropical convection, as continental and oceanic regimes may also differ in thermodynamic profile or larger-scale conditions otherwise. These considerations caution against interpreting our precise Darwin feature rankings or performance as universal.

However, initial inspection of "prediction ambiguity" as a qualifier on C-S state designations indicates that most of the C-S disagreement we observe is associated with conditions where radar signatures become less decisive (Figure 6). That relationship may seem intuitive, but is not guaranteed. Across the complete set of Darwin out-of-fold predictions, approximately 91% agree with the reference classification. For the ≈80% of columns having defined a relatively "low ambiguity" $A_i \leq 0.25$ condition, this agreement increases to 96% (e.g., Figure 7). In contrast, disagreement increases rapidly above $A_i = 0.25$, exceeding 30% at larger A_i. As with any imperfect problem, if our reference classifications are confidently "wrong", simple RF models may inherit those biases. For Darwin, only a small population (≈3%) disagree with our reference yet exhibit low ambiguity. These instances are instructive for downstream applications as they often expose situations where simple predictors conflict with assumptions imposed by the reference. To give an example, our reference classification enforces a "stratiform" designation for columns containing "bright band" signatures, even if faster falling media aloft strongly support a "convective" designation. Such a column will therefore be labelled as having a "disagreement" despite low ambiguity and without representing a clear failure of either designation.

https://doi.org/10.5194/egusphere-2026-6107
Preprint. Discussion started: 22 November 2026
© Author(s) 2026. CC BY 4.0 License.

Composite profiles (Figure 8) provide additional context for interpreting "prediction ambiguity" as a C-S qualifier. One question is whether prediction ambiguity simply reproduces loosely defined "transitional" precipitation used in previous C-S applications, or intermediary regions which have often been associated more closely with stratiform dynamical and microphysical processes (e.g., Houze, 1997; Schumacher et al., 2004). For Darwin, composite columns classified as "convective" by our reference (e.g., through the presence of faster falling media) retain appreciable median/mean air motions aloft (> 1 ms^{-1}) and lack pronounced bright band/aggregation structure even at higher A_i. Prediction ambiguity therefore tracks a progressive weakening of convective characteristics, but the composites do not show a corresponding emergence of characteristic stratiform process signatures. We also caution against interpreting weaker Z as "transitional" in convective contexts; our dataset includes isolated and organized convection having weak-Z peripheral regions that still may be associated with convective overturning and subsiding-shell motions (e.g., Giangrande et al., 2023; Mulhern et al., 2025). Stratiform composites similarly retain characteristic radar process signatures at higher A_i, although the more pronounced aggregation enhancements are associated with low ambiguity. Some separation between these populations necessarily reflects our reference classification, which assigns pronounced bright band columns as stratiform even when other convective signatures remain. Repeating these tests using the three-feature RF-predicted classifications produced similar overall patterns (not shown), although higher ambiguity populations exhibited greater mixing of dynamical/microphysical signatures between the regimes. Our intent was not to redefine "transitional" precipitation, but to quantify where and how strongly the radar information supporting a binary C-S designation becomes less distinct. For Darwin, increasing A_i captures this progression without implying that higher ambiguity convective precipitation has shifted predominantly stratiform.

Overall, we find that most Darwin columns occupy relatively low-ambiguity conditions having readily identifiable C-S characteristics, while a smaller portion occupies conditions where these distinctions become less pronounced. However, the meaning of higher ambiguity also differs between predicted C-S states. Stratiform predictions remain highly accurate until relatively large A_i, while higher ambiguity stratiform composites retain predominantly stratiform Z and air motion characteristics (Figure 8). In contrast, the accuracy of convective predictions decreases more steadily with increasing A_i. Physically, this is consistent with examples such as Figure 6 where simple predictors are confronted with competing information: elevated Z or Doppler signatures may support a "convective" designation even when a pronounced "bright band" favors stratiform. Such cases do not necessarily represent a clear failure of either C-S interpretation, particularly when faster falling media remain present aloft. A stratiform designation may reasonably represent the dominant precipitation structure, while those same columns may retain convective fall speed characteristics relevant to profiler air motion retrievals. Thus, the practical significance of C-S ambiguity may depend partly on the downstream application rather than on assuming a single boundary between the two states.

https://doi.org/10.5194/egusphere-2026-6107
Preprint. Discussion started: 22 November 2026
© Author(s) 2026. CC BY 4.0 License.

5 Conclusions and summary

This study uses observations from the dual-frequency Darwin wind profilers to investigate how effectively conventional radar measurements support convective-stratiform classifications (CSCs) and whether useful discrimination is uniquely tied to canonical radar signatures that have well-served this community. Random Forest algorithms provide an objective means for comparing how well individual and combined radar characteristics address these questions, rather than serving as an optimized classifier. Darwin profiler observations provide a unique perspective because vertical air motions and hydrometeor fall speeds retrieved from these systems allow reference CSC to be informed by the presence of faster falling, convectively processed media. Key findings are as follows:

- *Conventional reflectivity factor (Z) alone can support a highly capable convective-stratiform (C-S) distinction, but its value extends beyond precipitation intensity.* Height- and vertical structure-based features outperform column maximum Z, consistent with these quantities retaining information about the dynamical and microphysical processes shaping the precipitation column. Combinations of only a few such Z characteristics approach 0.90 balanced accuracy without velocity information.

- *A small number of complementary vertical-profile characteristics contribute sufficient information for highly capable C-S discrimination.* Lower-level (sub-melting layer) Z intensity, echo structure, and mean Doppler velocity (MDV) or spectral width (SW) provide complementary discriminatory information, with combinations exceeding 0.90 balanced accuracy. Most feature tests however encounter diminishing returns as additional characteristics are included.

- *Conventional Doppler measurements retain much of the C-S information available from direct hydrometeor fall speed (Vt).* Replacing |MDV|-Aloft with the more direct Vt-Aloft to establish the presence of faster falling media produces modest improvement, yet its relative advantage over MDV plateaus once complementary Z characteristics are included. Direct Vt insight does not appear necessary for high-fidelity CSC in these Darwin profiler applications.

- *Prediction ambiguity provides a useful qualifier on otherwise binary C-S designations.* Approximately 96% of low-ambiguity predictions agree with our Darwin reference, while disagreement rates exceed 30% within higher-ambiguity populations.

- *Higher-ambiguity populations generally retain characteristic C-S behavior, even as their radar and air motion distinctions become less pronounced.* Thus, this field may provide a continuous measure of where C-S distinctions weaken without requiring these conditions to be assigned to a separate “transitional” category.

https://doi.org/10.5194/egusphere-2026-6107
Preprint. Discussion started: 22 November 2026
© Author(s) 2026. CC BY 4.0 License.

For Darwin, these results provide a quantitative reference for how capable practical binary C-S classifications may be under relatively favorable observing conditions. Several relatively simple radar concepts recover the reference distinction at >90% skill despite known sampling limitations and the inherently fluid nature of C-S precipitation, providing a different view on C-S classification fidelity that has often been difficult to establish. These results suggest that the remaining challenge may be less about improving overall classification skill and more about identifying individual classifications for which the underlying C-S distinction is less clear. Most Darwin columns occupy relatively decisive states having readily identifiable C-S characteristics, whereas a smaller high-ambiguity population still retains recognizable C-S behavior when distinctions become less pronounced. Prediction ambiguity may therefore help reconcile the practical need for binary C-S designations with the expected continuum between these precipitation states. These ideas may also help identify conditions where the choice of C-S designation has greater consequences for downstream applications. Future efforts should determine whether these ambiguity relationships are portable to other profiler datasets and environments, and whether they can meaningfully characterize uncertainty in downstream C-S-dependent retrievals.

Code and data availability

The Darwin dual-frequency profiler datasets (processed, calibrated for the 2005-2006 monsoon season) are available through the BOM archive.

Supplement link

The link to the supplement will be included by Copernicus, if applicable.

Author contributions

AP, CW contributed to Darwin profiler dataset curation and troubleshooting/resources. SG, IS planned the initial concepts; SG developed the software, additional methodology and investigations. All authors contributed to the scientific discussion and to the writing (draft preparation, editing) of this paper.

Competing interests

The authors declare that they have no conflict of interest.

https://doi.org/10.5194/egusphere-2026-6107
Preprint. Discussion started: 22 November 2026
© Author(s) 2026. CC BY 4.0 License.

Acknowledgements

This paper has been authored by employees of Brookhaven Science Associates, LLC, under contract DE-SC0012704 with the U.S. DOE. Pacific Northwest National Laboratory is operated for the U.S. Department of Energy by Battelle (grant no. DE-AC05-76RL01830). The publisher by accepting the paper for publication acknowledges that the United States Government retains a nonexclusive, paid-up, irrevocable, worldwide license to publish or reproduce the published form of this paper, or allow others to do so, for United States Government purposes. We acknowledge support from the Atmospheric Radiation Measurement (ARM) program, a user facility of the U.S. DOE, Office of Science, sponsored by the Office of Biological and Environmental Research. Additional support was from the Atmospheric Systems Research (ASR) program of that office. ChatGPT (OpenAI) was used for technical editing and to assist with the development and refinement of analysis and visualization code. The authors would also like to thank David Mechem (KU) for thoughtful comments on this manuscript.

Financial support

This research has been supported by the US Department of Energy (grant no. DE-SC0012704, DE-AC05-76RL01830, DE-SC0021167, and DE-SC0025502).

References

Anagnostou, E. N.: A convective/stratiform precipitation classification algorithm for volume scanning weather radar observations, Meteorol. Appl., 11, 291–300, https://doi.org/10.1017/S1350482704001409, 2004.

Atlas, D., Ulbrich, C. W., Marks Jr., F. D., Black, R. A., Amitai, E., Willis, P. T., and Samsury, C. E.: Partitioning tropical oceanic convective and stratiform rains by draft strength, J. Geophys. Res., 105, 2259–2267, https://doi.org/10.1029/1999JD901009, 2000.

Biggerstaff, M. I. and Listemaa, S. A.: An Improved Scheme for Convective/Stratiform Echo Classification Using Radar Reflectivity, J. Appl. Meteorol., 39, 2129–2150, https://doi.org/10.1175/1520-0450(2001)040<2129:AISFCS>2.0.CO;2, 2000.

Borque, P., Kollias, P., and Giangrande, S.: First Observations of Tracking Clouds Using Scanning ARM Cloud Radars, J. Appl. Meteorol. Climatol., 53, 2732–2746, https://doi.org/10.1175/JAMC-D-13-0182.1, 2014.

Breiman, L.: Random forests, Mach. Learn., 45, 5–32, https://doi.org/10.1023/A:1010933404324, 2001.

Bringi, V. N., Chandrasekar, V., Hubbert, J., Gorgucci, E., Randeu, W. L., and Schoenhuber, M.: Raindrop size distribution in different climatic regimes from disdrometer and dual-polarized radar analysis, J. Atmos. Sci., 60, 354–365, https://doi.org/10.1175/1520-0469(2003)060<0354>2.0.CO;2, 2003.

Churchill, D. D. and Houze Jr., R. A.: Development and structure of winter monsoon cloud clusters on 10 December 1978, J. Atmos. Sci., 41, 933–960, https://doi.org/10.1175/1520-0469(1984)041<0933>2.0.CO;2, 1984.

https://doi.org/10.5194/egusphere-2026-6107
Preprint. Discussion started: 22 November 2026
© Author(s) 2026. CC BY 4.0 License.



Dixon, M. and Romatschke, U.: Three-Dimensional Convective–Stratiform Echo-Type Classification and Convectivity Retrieval from Radar Reflectivity, J. Atmos. Oceanic Technol., 39, 1685–1704, https://doi.org/10.1175/JTECH-D-22-0018.1, 2022.

Fabry, F. and Zawadzki, I.: Long-Term Radar Observations of the Melting Layer of Precipitation and Their Interpretation, J. Atmos. Sci., 52, 838–851, https://doi.org/10.1175/1520-0469(1995)052<0838:LTROOT>2.0.CO;2, 1995.

Gagne II, D. J., McGovern, A., and Xue, M.: Machine learning enhancement of storm-scale ensemble probabilistic quantitative precipitation forecasts, Weather Forecast., 29, 1024–1043, https://doi.org/10.1175/WAF-D-13-00108.1, 2014.

Gagne II, D. J., McGovern, A., Haupt, S. E., Sobash, R. A., Williams, J. K., and Xue, M.: Storm-based probabilistic hail forecasting with machine learning applied to convection-allowing ensembles, Weather Forecast., 32, 1819–1840, https://doi.org/10.1175/WAF-D-17-0010.1, 2017.

Gamache, J. F. and Houze Jr., R. A.: Water budget of a mesoscale convective system in the tropics, J. Atmos. Sci., 40, 1835–1850, https://doi.org/10.1175/1520-0469(1983)040<1835>2.0.CO;2, 1983.

Geerts, B. and Dawei, Y.: Classification and Characterization of Tropical Precipitation Based on High-Resolution Airborne Vertical Incidence Radar. Part I: Classification, J. Appl. Meteorol. Climatol., 43, 1554–1566, https://doi.org/10.1175/JAM2158.1, 2004.

Geurts, P., Ernst, D., and Wehenkel, L.: Extremely randomized trees, Mach. Learn., 63, 3–42, https://doi.org/10.1007/s10994-006-6226-1, 2006.

Ghada, W., Casellas, E., Herbinger, J., Garcia-Benadí, A., Bothmann, L., Estrella, N., Bech, J., and Menzel, A.: Stratiform and Convective Rain Classification Using Machine Learning Models and Micro Rain Radar, Remote Sens., 14, 4563, https://doi.org/10.3390/rs14184563, 2022.

Giangrande, S. E. and Ryzhkov, A. V.: Estimation of Rainfall Based on the Results of Polarimetric Echo Classification, J. Appl. Meteorol. Climatol., 47, 2445–2462, https://doi.org/10.1175/2008JAMC1753.1, 2008a.

Giangrande, S. E., Krause, J. M., and Ryzhkov, A. V.: Automatic Designation of the Melting Layer with a Polarimetric Prototype of the WSR-88D Radar, J. Appl. Meteorol. Climatol., 47, 1354–1364, https://doi.org/10.1175/2007JAMC1634.1, 2008b.

Giangrande, S. E., Luke, E. P., and Kollias, P.: Characterization of Vertical Velocity and Drop Size Distribution Parameters in Widespread Precipitation at ARM Facilities, J. Appl. Meteorol. Climatol., 51, 380–391, https://doi.org/10.1175/JAMC-D-10-05000.1, 2012.

Giangrande, S. E., Collis, S., Straka, J., Protat, A., Williams, C., and Krueger, S.: A Summary of Convective-Core Vertical Velocity Properties Using ARM UHF Wind Profilers in Oklahoma, J. Appl. Meteorol. Climatol., 52, 2278–2295, https://doi.org/10.1175/JAMC-D-12-0185.1, 2013.

Giangrande, S. E., Bartholomew, M. J., Pope, M., Collis, S., and Jensen, M. P.: A Summary of Precipitation Characteristics from the 2006–11 Northern Australian Wet Seasons as Revealed by ARM Disdrometer Research Facilities (Darwin, Australia), J. Appl. Meteorol. Climatol., 53, 1213–1231, https://doi.org/10.1175/JAMC-D-13-0222.1, 2014.

https://doi.org/10.5194/egusphere-2026-6107
Preprint. Discussion started: 22 November 2026
© Author(s) 2026. CC BY 4.0 License.

Giangrande, S. E., Toto, T., Jensen, M. P., Bartholomew, M. J., Feng, Z., Protat, A., Williams, C. R., Schumacher, C., and Machado, L.: Convective cloud vertical velocity and mass-flux characteristics from radar wind profiler observations during GoAmazon2014/5, J. Geophys. Res.-Atmos., 121, 12891–12913, https://doi.org/10.1002/2016JD025303, 2016.

Giangrande, S. E., Biscaro, T. S., and Peters, J. M.: Seasonal controls on isolated convective storm drafts, precipitation intensity, and life cycle as observed during GoAmazon2014/5, Atmos. Chem. Phys., 23, 5297–5316, https://doi.org/10.5194/acp-23-5297-2023, 2023.

Giangrande, S. E., Williams, C. R., and Protat, A.: Dual-frequency profiler study of hydrometeor fall speeds in tropical deep convection, EGUsphere [preprint], https://doi.org/10.5194/egusphere-2026-856, 2026.

Heinselman, P. L. and Ryzhkov, A. V.: Validation of Polarimetric Hail Detection, Wea. Forecasting, 21, 839–850, https://doi.org/10.1175/WAF956.1, 2006.

Houze Jr., R. A.: Observed structure of mesoscale convective systems and implications for large-scale heating, Q. J. Roy. Meteor. Soc., 115, 425–461, https://doi.org/10.1002/qj.49711548702, 1989.

Houze Jr., R. A.: Cloud Dynamics, Academic Press, San Diego, USA, 573 pp., 1993.

Houze Jr., R. A.: Stratiform precipitation in regions of convection: A meteorological paradox?, Bull. Amer. Meteor. Soc., 78, 2179–2196, https://doi.org/10.1175/1520-0477(1997)078<2179>2.0.CO;2, 1997.

Johnson, R. H., Rickenbach, T. M., Rutledge, S. A., Ciesielski, P. E., and Schubert, W. H.: Trimodal characteristics of tropical convection, J. Climate, 12, 2397–2418, https://doi.org/10.1175/1520-0442(1999)012<2397>2.0.CO;2, 1999.

Kumar, V. V., Jakob, C., Protat, A., Williams, C. R., and May, P. T.: Mass-flux characteristics of tropical cumulus clouds from wind profiler observations at Darwin, Australia, J. Atmos. Sci., 72, 1837–1855, https://doi.org/10.1175/JAS-D-14-0259.1, 2015.

Kumar, V. V., Protat, A., Jakob, C., Williams, C. R., Rauniyar, S., Stephens, G. L., and May, P. T.: The estimation of convective mass flux from radar reflectivities, J. Appl. Meteorol. Climatol., 55, 1239–1257, https://doi.org/10.1175/JAMC-D-15-0193.1, 2016.

Kumjian, M. R., Mishra, S., Giangrande, S. E., Toto, T., Ryzhkov, A. V., and Bansemer, A.: Polarimetric radar and aircraft observations of saggy bright bands during MC3E, J. Geophys. Res. Atmos., 121, 3584–3607, https://doi.org/10.1002/2015JD024446, 2016.

Lang, S., Tao, W., Simpson, J., and Ferrier, B.: Modeling of convective–stratiform precipitation processes: Sensitivity to partitioning methods, J. Appl. Meteorol., 42, 505–527, https://doi.org/10.1175/1520-0450(2003)042<0505>2.0.CO;2, 2003.

Lerach, D. G., Rutledge, S. A., Williams, C. R., and Cifelli, R.: Vertical Structure of Convective Systems during NAME 2004, Mon. Weather Rev., 138, 1695–1714, https://doi.org/10.1175/2009MWR3053.1, 2010.

Mecikalski, J. R., Sandmæl, T. N., Murillo, E. M., Homeyer, C. R., Bedka, K. M., Apke, J. M., and Jewett, C. P.: A random-forest model to assess predictor importance and nowcast severe storms using high-resolution radar–GOES satellite–lightning observations, Mon. Weather Rev., 149, 1725–1746, https://doi.org/10.1175/MWR-D-19-0274.1, 2021.

https://doi.org/10.5194/egusphere-2026-6107
Preprint. Discussion started: 22 November 2026
© Author(s) 2026. CC BY 4.0 License.

Mulhern, Q. R., Peters, J. M., and Mulholland, J. P.: Driving Mechanisms for Subsiding Shells in Simulations of Deep Moist Convection, EGUsphere [preprint], https://doi.org/10.5194/egusphere-2025-4495, 2025.

Pedregosa, F., Varoquaux, G., Gramfort, A., Michel, V., Thirion, B., Grisel, O., Blondel, M., Prettenhofer, P., Weiss, R., Dubourg, V., Vanderplas, J., Passos, A., Cournapeau, D., Brucher, M., Perrot, M., and Duchesnay, É.: Scikit-learn: Machine learning in Python, J. Mach. Learn. Res., 12, 2825–2830, 2011.

Powell, S. W., Houze, R. A., and Brodzik, S. R.: Rainfall-Type Categorization of Radar Echoes Using Polar Coordinate Reflectivity Data, J. Atmos. Oceanic Technol., 33, 523–538, https://doi.org/10.1175/JTECH-D-15-0135.1, 2016.

Protat, A. and Williams, C. R.: The accuracy of radar estimates of ice terminal fall speed from vertically pointing Doppler radar measurements, J. Appl. Meteorol. Climatol., 50, 2120–2138, https://doi.org/10.1175/JAMC-D-10-05031.1, 2011.

Schumacher, C., Houze, R. A., and Kraucunas, I.: The Tropical Dynamical Response to Latent Heating Estimates Derived from the TRMM Precipitation Radar, J. Atmos. Sci., 61, 1341–1358, https://doi.org/10.1175/1520-0469(2004)061<1341:TTDRTL>2.0.CO;2, 2004.

Schumacher, C., Zhang, M. H., and Ciesielski, P. E.: Heating structures of the TRMM field campaigns, J. Atmos. Sci., 64, 2593–2610, https://doi.org/10.1175/JAS3938.1, 2007.

Schumacher, C., Stevenson, S. N., and Williams, C. R.: Vertical motions of the tropical convective cloud spectrum over Darwin, Australia, Q. J. R. Meteorol. Soc., 141, 2277–2288, https://doi.org/10.1002/qj.2520, 2015.

Shige, S., Takayabu, Y. N., Tao, W., and Johnson, D. E.: Spectral retrieval of latent heating profiles from TRMM PR data. Part I: Development of a model-based algorithm, J. Appl. Meteorol., 43, 1095–1113, https://doi.org/10.1175/1520-0450(2004)043<1095>2.0.CO;2, 2004.

Steiner, M., Houze Jr., R. A., and Yuter, S. E.: Climatological characterization of three-dimensional storm structure from operational radar and rain gauge data, J. Appl. Meteorol., 34, 1978–2007, https://doi.org/10.1175/1520-0450(1995)034<1978>2.0.CO;2, 1995.

Tao, W., Iguchi, T., and Lang, S.: Expanding the Goddard CSH algorithm for GPM: New extratropical retrievals, J. Appl. Meteorol. Climatol., 58, 921–946, https://doi.org/10.1175/JAMC-D-18-0215.1, 2019.

Tian, L., Heymsfield, G. M., Li, L., and Srivastava, R. C.: Properties of light stratiform rain derived from 10- and 94-GHz airborne Doppler radars measurements, J. Geophys. Res.-Atmos., 112, D11211, https://doi.org/10.1029/2006JD008144, 2007.

Tokay, A. and Short, D. A.: Evidence from Tropical Raindrop Spectra of the Origin of Rain from Stratiform versus Convective Clouds, J. Appl. Meteorol., 35, 355–371, https://doi.org/10.1175/1520-0450(1996)035<0355:EFTRSO>2.0.CO;2, 1996.

Wang, D., Giangrande, S. E., Bartholomew, M. J., Hardin, J., Feng, Z., Thalman, R., and Machado, L. A. T.: The Green Ocean: precipitation insights from the GoAmazon2014/5 experiment, Atmos. Chem. Phys., 18, 9121–9145, https://doi.org/10.5194/acp-18-9121-2018, 2018.

Wang, D., Giangrande, S. E., Schiro, K., Jensen, M. P., and Houze, R. A.: The characteristics of tropical and midlatitude mesoscale convective systems as revealed by radar wind profilers, J. Geophys. Res.-Atmos., 124, 4601–4619, https://doi.org/10.1029/2018JD030087, 2019.

https://doi.org/10.5194/egusphere-2026-6107
Preprint. Discussion started: 22 November 2026
© Author(s) 2026. CC BY 4.0 License.



Wang, D., Giangrande, S. E., Feng, Z., Hardin, J. C., and Prein, A. F.: Updraft and Downdraft Core Size and Intensity as Revealed by Radar Wind Profilers: MCS Observations and Idealized Model Comparisons, J. Geophys. Res.-Atmos., 125, e2019JD031774, https://doi.org/10.1029/2019JD031774, 2020a.

Wang, D., Jensen, M. P., D'Iorio, J. A., Jozef, G., Giangrande, S. E., Johnson, K. L., and Bartholomew, M. J.: An observational comparison of level of neutral buoyancy and level of maximum detrainment in tropical deep convective clouds, J. Geophys. Res.-Atmos., 125, e2020JD032637, https://doi.org/10.1029/2020JD032637, 2020b.

Williams, C. R., Ecklund, W. L., and Gage, K. S.: Classification of Precipitating Clouds in the Tropics Using 915-MHz Wind Profilers, J. Atmos. Oceanic Technol., 12, 996–1012, https://doi.org/10.1175/1520-0426(1995)012<0996:COPCIT>2.0.CO;2, 1995.

Williams, C. R.: Vertical air motion retrieved from dual-frequency profiler observations, J. Atmos. Oceanic Technol., 29, 1471–1480, https://doi.org/10.1175/JTECH-D-11-00176.1, 2012.

Yang, Z., Liu, P., and Yang, Y.: Convective/Stratiform Precipitation Classification Using Ground-Based Doppler Radar Data Based on the K-Nearest Neighbor Algorithm, Remote Sens., 11, 2277, https://doi.org/10.3390/rs11192277, 2019.